Journal of Chromatography, 191 (1980) 47–60

CHROM. 12,346

POLAROGRAPHIC DETECTION FOR HIGH-PERFORMANCE LIQUID CHROMATOGRAPHY USING A FLOW-THROUGH DETECTOR

WŁODZIMIERZ KUTNER, JANUSZ DĘBOWSKI and WIKTOR KEMULA

Institute of Physical Chemistry of the Polish Academy of Sciences, Kasprzaka 44/52, 01-224 Warsaw (Poland)

SUMMARY

A new arrangement of a flow-through polarographic detector has been designed with a rapidly dropping mercury electrode. The detector is especially usefull for reversed-phase high-performance liquid chromatography (HPLC). It has been shown that the properties of the detector are similar to those of a UV detector operated at 254 nm. An electroactive substance in the eluate can be determined at flow-rates not exceeding 6 ml min^{-1}. An upwards direction of flow of the solution facilitates the automatic removal of gas bubbles, which are swept to the detector with the column effluent. The volume of solution necessary to wash out 95% of the detection passage filled with another solution is about 0.1 ml, which is approximately equal to the volume when using a UV (254 nm) detector with a geometrical volume of the detection passage of 8 μl. The detector sensitivity with injection of cadmium nitrate solution is $(3.6 \pm 0.4) \cdot 10^{-4}$ A l mol^{-1}, and the linear dynamic range is $5 \cdot 10^{-4}$–$5 \cdot 10^{-2}$ M cadmium nitrate with 5-μl injections. The selection of a suitably short drop time at a given flow-rate enables one to eliminate current signal disturbances on the recorded curves. Thus the current is diffusion or convective-diffusion controlled, irrespective of the presence or absence of turbulence. The application of the detector to HPLC is illustrated with the separation of a mixture of testosteroids.

INTRODUCTION

The dropping mercury electrode (DME) has been used succesfully for many years in devices for the detection of electroactive substances in a flowing electrolyte[1–21]. This electrode is particularly useful for monitoring an injected substance in the eluate from a chromatographic column in reversed-phase liquid chromatography[22,23]. Many different arrangements of polarographic detectors for liquid[1,4,6,7,12,15–17,19–21] and gas chromatography[13,14] have been described. The polarographic detector is a specific detector, the selectivity of which is controlled by the applied potential. High-performance liquid chromatography (HPLC) imposes new requirements on polarographic detection conditions. The flow-rate of the mobile phase is several orders of magnitude higher than that in classical liquid chromatography, and accordingly, the detection

volume must be as small as possible in order to prevent peak broadening. When polarographic detection is used, the signal height is dependent on the rate of mass transport of the studied substance to the electrode surface. A reduction of the dimensions of the detection chamber at a given flow-rate leads to an increase in the linear flow-rate up to turbulent flow. If turbulence occurs a reliable polarographic experiment is no longer possible. Although workers who have described flow-through polarographic detectors for HPLC realized these difficulties[15–17,19–21], the problem has not been discussed in detail.

In recent years, increasing attention has been paid to flow-through voltammetric detectors (for a review see, *e.g.*, refs. 24–26). Solid electrodes have the virtue of usually having greater positive potential limits of polarizability than mercury, which enables one to perform oxidation processes with several organic compounds, and they are also easy to handle. However, they have several shortcomings. The negative potential limit is usually poorer than that with mercury. The height of a chromatographic peak is unfortunately potential dependent owing to the presence of potential-dependent residual currents[27]. The advantages of the DME, such as the high limits of negative polarization potentials and the continuously renewing surface, which ensures a high reproducibility, have stimulated the further development of detectors with this type of electrode. Also, the DME, with which it is easy to measure the changes in differential capacity of the electrical double layer, enables one to determine electroinactive surfactants in column effluents[28–31], which makes the detector more universal.

In previously described flow-through polarographic detectors, dropping mercury electrodes with both normal and short drop times have been used[8,9,11,18]. The latter are particularly useful in flow-through systems at high linear flow-rates, although they are also advantageous in non-flowing systems[32]. In the detector described in this paper, a rapidly dropping mercury electrode (RDME) is used. The new detector can maintain reproducible conditions of polarographic measurement at a minimal detection volume. We present also the method of testing the performance of the flow-through detector, *i.e.*, we discuss the hydrodynamic conditions under which polarographic detection is possible and gives the best results.

EXPERIMENTAL

Apparatus and reagents

Analytical-reagent grade chemicals and doubly distilled water were used, except for acetonitrile, which was of technical grade. Steroids were obtained from Merck (Darmstadt, G.F.R.). As supporting electrolytes 0.1 *M* potassium nitrate and 1/15 *M* phosphate buffer (pH 6) according to Michaelis were used.

A home-made high-performance liquid chromatograph was used, consisting of two syringe pumps, programming and pump control units, pressure gauge with a ferrite pressure transducer[33], and a UV detector (254 nm) with a Z-shaped detection passage with a geometric volume of 8 μl. Chromatograms were recorded with the use of a Sefram (France) *Y–t* recorder. A 250 × 4 mm I.D. stainless-steel column was used, slurry packed at 300 kg cm^{-2} with LiChrosorb RP-18 (10 μm) octadecylsilane reversed-phase packing material (Merck).

Polarographic measurements were carried out with a Radelkis OH-102

(Hungary) polarograph. For the measurement of current–time curves at single mercury drops a circuit composed of a Chemipan PS-8 (Poland) potentiostat and a Tektronix 5103N storage oscilloscope with a 5A2ON differential amplifier was utilized.

Detector design

The detector design (Fig.1), based to a certain extent on previous designs[1,11,18,19,21], was especially aimed at reducting the effective detection volume and effecting automatic removal of gas bubbles from the detection space[34].

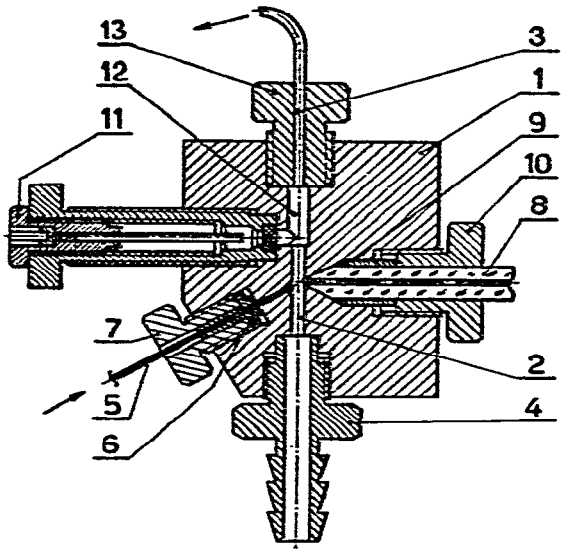

Fig. 1. Flow-through polarographic detector. 1 = Body; 2 = detection passage; 3 = waste solution capillary; 4 = clamping sleeve to mercury connector tube; 5 = solution inlet capillary; 6 = inlet capillary fastening ring gasket; 7 = inlet capillary clamping sleeve; 8 = RDME; 9 = RDME fastening sleeve; 10 = RDME clamping sleeve; 11 = Ag/AgCl reference electrode; 12 = degassing passage; 13 = waste solution capillary fastening sleeve.

There is a two-stage cylindrical chamber, in the PTFE body of the detector, which consists of the detection passage in the lower part (2 mm I.D.) and a degassing passage in the upper part (4 mm I.D.). The column eluate is fed to the detection passage with the use of a stainless-steel inlet capillary (0.2 mm I.D., 10 cm long). The inlet capillary is situated at 60° to the axis of the passage in order to eliminate backwards mixing of a passing solution in the space between the bottom of the mercury and the RDME. Such mixing could lead to the diffusion of a sample. The nozzle of the inlet capillary is located in the vicinity of the tip of the RDME.

The detector operates with a three-electrode system. The working electrode is the RDME (capillary length 65 mm, $m = 4.42$ mg sec^{-1} at $h_{Hg} = 80$ cm in 0.1 M potassium nitrate solution). Its drop time, t_1, is independent of the mobile phase flow-rate for $t_1 \leqslant 0.6$ sec. The RDME is situated perpendicular to the axis of the detection passage, which makes the drop time shorter[35]. The polarographic capillary tip is conically tapered for tightening the detector. The drop time was controlled in the range from 0.1 to 1.0 sec by changing the height of the mercury column and also

by revolution of the whole detector round the axis perpendicular to the axis of the detection passage and the RDME. The drop time of a capillary situated horizontally is one quarter of the drop time of the same capillary situated vertically[5]. It appeared in practice that the best working conditions were achieved when the polarographic capillary worked at an angle of approximately 30° to the horizontal.

The auxiliary electrode consists of the bottom of the mercury, which simultaneously shuts off hydraulically the detection passage at the bottom. An Ag/AgCl electrode filled with saturated sodium chloride solution is used as the reference electrode, situated downstream, *i.e.*, higher than the RDME, and is separated from the passing solution with a sintered-glass frit of porosity 4.

The solution flows upwards inside the detector. Although in this instance turbulence occurs at a lower flow-rate than with the opposite flow direction[2], it is more convenient for carrying away gas bubbles swept into the detector with the column eluate. Removal of gas bubbles was occasionally assisted by rhythmic squeezing of the tube containing mercury as the auxiliary electrode.

Procedure

The mobile phase solution was deaerated by purging with argon and then degassed at an ultrasonic bath. The argon was first purged by washing with a solution of the same composition as the mobile phase. The chromatographic column was conditioned before use by passing through it about 100 ml of mobile phase solution. The sample or the solution under test was injected at the top of the column with a 5-μl sample injection valve.

RESULTS AND DISCUSSION

Performance of detector

Detection volume. One of the most fundamental requirements is a small detection volume. In a polarographic detector, in which current detection signal is determined by the rate of mass transport of a substance being reduced or oxidized at the electrode surface, the geometric volume of the detection passage does not determine unequivocally the solution volume in which detection occurs. This is why we used the so-called "effective detection volume" to compare the detection volume of our detector with that of UV (254 nm) detector. As a measure of the effective detection volume we consider volume of solution that has to be passed through the detector in order to wash up to 95% of the original solution at flow-rate $v^* \rightarrow 0$ ml min^{-1}. The experiment, similar to that described previously[10,11,18,35] is outlined schematically in Fig. 2a.

One of the pumps of the chromatograph was filled with 0.1 *M* potassium nitrate solution and the other with 10^{-3} *M* cadmium nitrate in 0.1 *M* potassium nitrate solution. The RDME was kept at the potential of the plateau of the Cd^{2+} reduction wave, $E = -0.9$ V *vs.* Ag/AgCl. The pumps were connected to the polarographic detector through a six position stopcock (PTFE rotatory valve; Jobling, Great Britain), which facilitated changeover of the solution jet without changing its flow-rate. As the wash time, Δt, a mean time was taken in which the solution filling the detector is up to 95% removed, *i.e.*, the time at which the current reaches 95% of its limiting value when the solution jet is altered from 0.1 *M* potassium nitrate solution to $5 \cdot 10^{-3}$ *M* cadmium nitrate in 0.1 *M* potassium nitrate solution and back. When

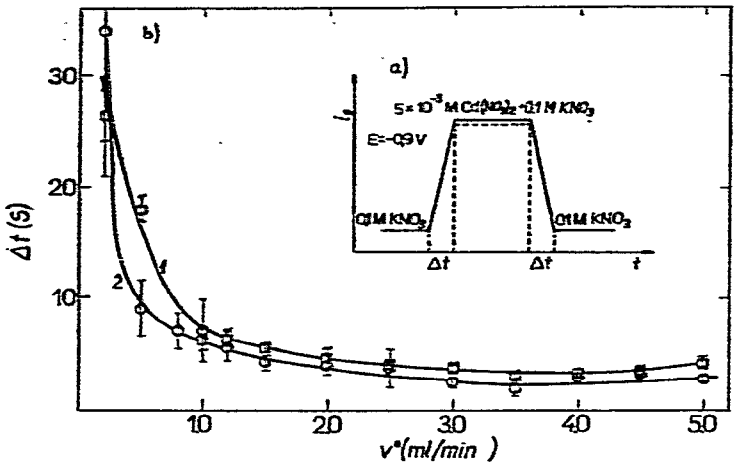

Fig. 2. Determination of time of washing-out to the extent of 95% with (1) UV (254 nm) and (2) polarographic detector. (a) Experimental scheme; concentrations on the curve refer to polarographic detector experiment; i_g, limiting current; (b) washing-out time as a function of solution flow-rate.

the UV (254 nm) detector was used in a similar experiment, one pump was filled with water and another with 10^{-3} *M* cadmium nitrate in 0.1 *M* potassium nitrate solution. The results for both detectors as a function of the solution flow-rate are presented in Fig. 2b. Based on these results, the effective detection volume, v ($v = \Delta t \cdot v^*$), which is presented as a function of flow-rate in Fig. 3, was calculated.

Extrapolation of the curves in Fig. 3 to $v^* = 0$ ml min^{-1} for both detectors gives an effective detection volume of *ca.* 0.1 ml. For the polarographic detector this volume appeared to be independent of the distance of the actual position of the bottom of the mercury from the outlet of polarographic capillary. Therefore, the volume below the RDME does not influence the effective detection volume. From this experiment, it can be concluded that the polarographic detector does not intro-

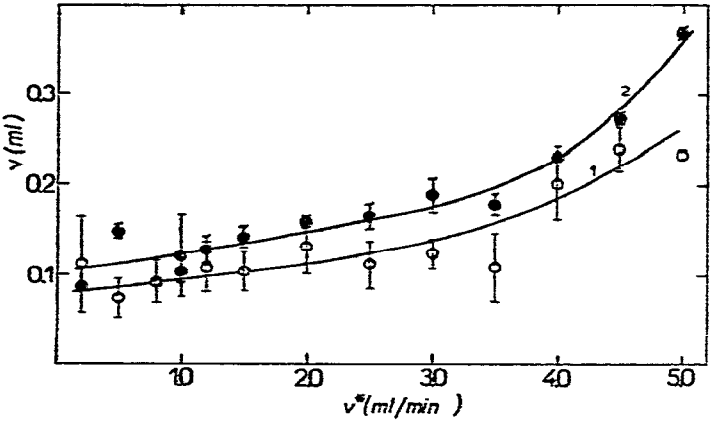

Fig. 3. Washing-out volume ($v = v^* \Delta t$) to 95% of signal height as a function of solution flow-rate for (1) polarographic and (2) UV (254 nm) detector.

duce greater signal broadening, at least in the frontal method, than UV detectors, in spite of the difference in the geometries of their detection passages.

Hydrodynamic conditions and transport control. Measurements of the dependence of the limiting current on flow-rate at different drop times, controlled by the height of the mercury, were performed in order to elucidate the influence of hydrodynamic conditions on the signal height. As can be seen from Fig. 4, the limiting current for 10^{-3} *M* cadmium nitrate in 0.1 *M* potassium nitrate solution is hardly dependent on flow-rate for $t_1 \leqslant 0.2$ sec, but the limiting current is the higher the longer is the drop time and the higher is the flow-rate. However, for too long drop times ($t_1 \geqslant 0.8$ sec) and high flow-rates, disturbances and irreproducible values of the limiting current were observed. This effect could originate from turbulence of the solution flow. To check this possibility the flow conditions in the inlet capillary of inner diameter $D = 0.2$ mm and the detection passage of $D = 2$ mm were estimated.

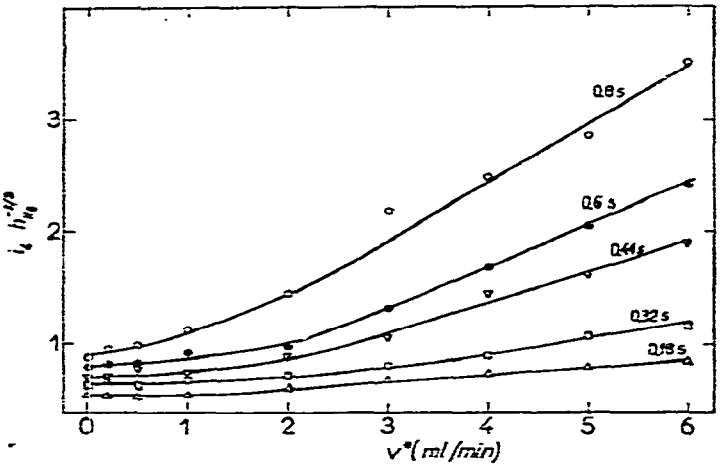

Fig. 4. Dependence of limiting current for 10^{-3} *M* $Cd(NO_3)_2$ in 0.1 *M* KNO_3 solution on electrolyte flow-rate for different drop times of RDME. Drop time in seconds is given on each curve. i_l, limiting current.

In Table I, values of Reynolds numbers, $Re = D\eta\varrho/\mu$, are presented for a given linear flow-rate, η, taking the density, ϱ, and dynamic viscosity, μ, of the solution to be equal to those of pure water at room temperature ($\varrho = 1.0045 \cdot 10^3$ kg sec^{2}m^{-2}, $\mu = 0.9044 \cdot 10^{-4}$ kg sec m^{-2}). It follows from Table I that laminar flow ($Re \leqslant 2100$) may be expected for a flow-rate of $v^* \leqslant 2$ ml min^{-1}. The linear flow-rate of mercury in the RDME at the mercury flow-rate used was of the order of 1 m sec^{-1}. This value is considerably smaller than the solution linear flow-rate in the inlet capillary, and hence the mercury flow should not be a source of turbulence.

The conclusion about turbulent flow was verified experimentally by measurement of the instantaneous current–time curves at a single mercury drop for different electrolyte flow-rates.

As can be seen in Fig. 5, these curves for $5 \cdot 10^{-3}$ *M* cadmium nitrate in 0.1 *M* potassium nitrate solution show that there is a distinct increase in current with

TABLE I

REYNOLDS NUMBER FOR DIFFERENT FLOW-RATES IN THE INLET CAPILLARY AND DETECTION PASSAGE OF THE DETECTOR

v^* (ml min^{-1})	$D = 0.2 \cdot 10^{-3}$ m		$D = 2 \cdot 10^{-3}$ m	
	$\eta \times 10^3$ (m sec^{-1})	Re	$\eta \times 10$ (m sec^{-1})	Re
0.1	5.3	118	0.053	11.8
0.2	10.6	235	0.106	23.5
0.5	26.5	590	0.265	59.0
1.0	53.0	1180	0.531	118
2.0	106.0	2350	1.062	235
3.0	159.2	3532	1.592	353
4.0	212.3	4692	2.123	469
5.0	265.4	5895	2.654	590
6.0	318.5	7075	3.185	708

increase in flow-rate for a given drop time. In contrast to the work of Tamamushi *et al.*[9], where the linear liquid flow-rate did not exceed 9 cm sec^{-1}, turbulence was observed only for flow-rates of $v^* \geqslant 5$ ml min^{-1}. Therefore, the experiments gave better results than could be predicted from Table I. However, for such high values of the flow-rate, the turbulence effect can be eliminated only if the drop time is short enough. Then, for lower flow-rates and $t_1 \leqslant 0.20$ sec, a change in flow-rate

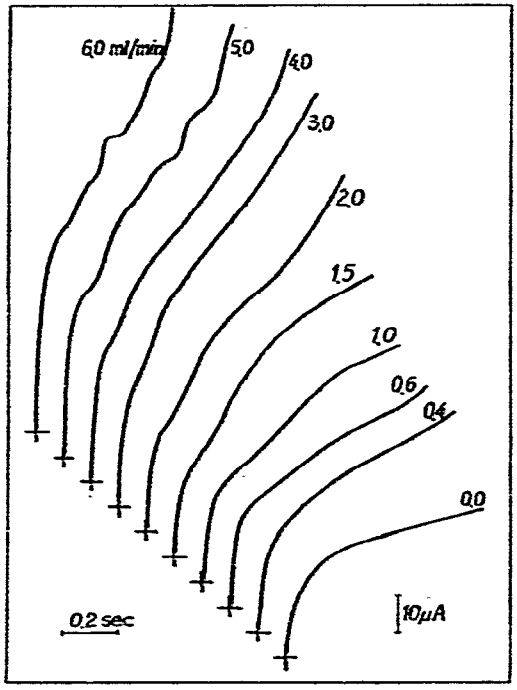

Fig. 5. Current–time curves at a single mercury drop for the solution containing $5 \cdot 10^{-3}$ *M* $Cd(NO_3)_2$ in 0.1 *M* KNO_3 at potential $E = -1.0$ V *vs.* SCE. Flow-rate (ml min^{-1}) is given on each curve. The polarographic capillary was situated at 45° to the horizontal.

virtually does not influence the current. This indicates that for such short drop times the thickness of the diffusion layer is less than the thickness of the convective layer and the current remains under diffusion control, irrespective of the presence of convective transport. Such a conclusion might already be drawn on the basis of the curve for $t_1 = 0.18$ sec in Fig. 4.

This conclusion can also be discussed on the basis of the analysis of the dependence of the logarithm of the limiting current (normalized for the mercury column height) on the logarithm of the drop time for 10^{-3} *M* cadmium nitrate in 0.1 *M* potassium nitrate solution for different electrolyte flow-rates (Fig. 6) and the dependence of the logarithm of the limiting current on the logarithm of the mercury column height for different flow-rates for 10^{-3} *M* cadmium nitrate in 0.1 *M* potassium nitrate solution (Fig. 7).

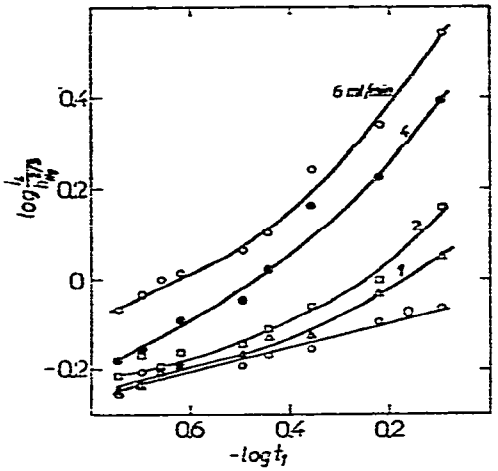

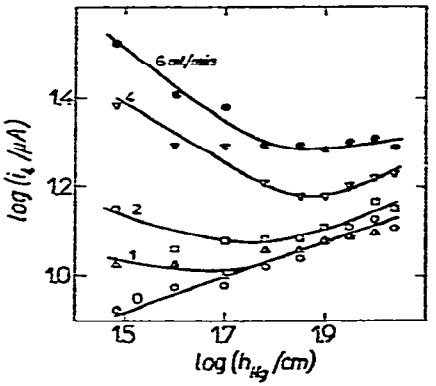

Fig. 6. Dependence of logarithm of limiting current on logarithm of drop time for different electrolyte flow-rates for 10^{-3} *M* $Cd(NO_3)_2$ in 0.1 *M* KNO_3 solution. Flow-rate (ml min^{-1}) is given on each curve.

Fig. 7. Dependence of logarithm of limiting current on logarithm of the mercury column height for 10^{-3} *M* $Cd(NO_3)_2$ in 0.1 *M* KNO_3 solution. Flow-rate (ml min^{-1}) is given on each curve.

For $v^* = 0$ ml min^{-1}, the slope of the curves in Fig. 6 is $\partial \log(i_1 h_{Hg}^{-2/3})/\partial \log t_1 = 0.27$. This value is higher than 0.17, which is characteristic of diffusion-controlled processes[37]. This difference might be caused by effects of formation of polarographic maxima of the second kind on the Cd^{2+} reduction wave, particularly with short drop times[9]. With an increase in v^* this slope increased and for $v^* \geqslant 4$ ml min^{-1} and $t_1 \leqslant 0.44$ sec was equal to 0.45, which is close to 4/9, which is characteristic of currents limited by laminar convection[17]. More than doubled values of the slope of the curves for $v^* > 4$ ml min^{-1} and $t_1 > 0.44$ sec may indicate the presence of turbulence.

For $v^* = 0$ ml min^{-1} the slope of the curves in Fig. 7 is $\partial \log i_1/\partial \log h_{Hg} = 0.44$, which is close to the value of 0.5, characteristic of diffusion-controlled processes. With an increase in solution flow-rate this slope decreases for lower values of mercury column height, that is, for longer drop times, and eventually, for $v^* \geqslant 2$ ml min^{-1},

it becomes negative, indicating convective transport control. At higher h_{Hg} values, *i.e.*, shorter t_1, the process remains under diffusion control, maintaining a positive slope of the curves.

In addition to the application of the shorter drop time method, turbulence at higher flow-rates might be eliminated, of course, by suitable modelling of the cell shape[2]. This would lead to an increase in the volume of the detection chamber, which at a fixed flow-rate would decrease the linear flow-rate in the vicinity of the DME. However, this would result in peak broadening.

Chromatographic characteristics of the detector. The linear dynamic range was studied by the injection into flowing supporting electrolyte (0.1 *M* potassium nitrate solution) a 5-μl volume of cadmium nitrate solution of 11 different concentrations in the range from $5 \cdot 10^{-5}$ to 0.1 *M* in 0.1 *M* potassium nitrate solution (Fig. 8).

The lower limit of the linear dynamic range was close to $5 \cdot 10^{-4}$ *M* cadmium nitrate, and was mainly determined by the accuracy of deaeration of the sample solution and mobile phase and the stability of the pump efficiency. The noise was *ca.* $2 \cdot 10^{-8}$ A. The upper limit of the linear dynamic range was $5 \cdot 10^{-2}$ *M*. It was possible to achieve this relatively high value by the application of a three-electrode system with the elimination of potential ohmic loss. The dependence of the peak area, S (μC) on the concentration (C) of injected sample presented in Fig. 8 can be described by the equation

$$S = S_0 + k\,C^n \qquad (1)$$

where S_0 = residual charge, k = detector sensitivity and n = detector response. For our detector n, calculated as the slope of the curve in Fig. 8, is equal unity, independent of the flow-rate. The detector sensitivity, obtained by the extrapolation of the curves in Fig. 8 to the value $\log C_{Cd^{2+}} = 0$, decreases with increase in flow-rate (Table II), as has been observed previously[16].

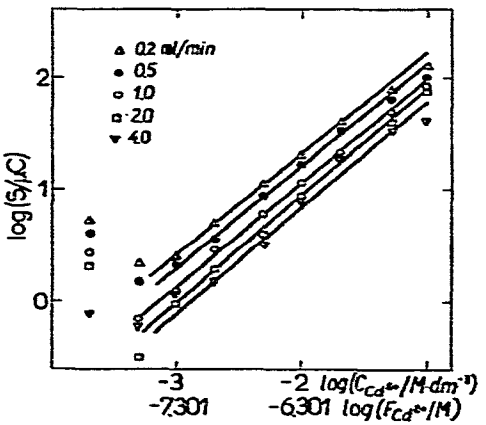

Fig. 8. Dependence of logarithm of the peak surface area, S [$S = W_{1/2}$ (sec) · h(μA)], on logarithm of concentration, or number of moles, F, of a 5-μl injected sample of $Cd(NO_3)_2$ in 0.1 *M* KNO_3 solution as mobile phase for different electrolyte flow-rates without a chromatographic column; $t_1 = 0.22 \pm 0.02$ sec, $h_{Hg} = 110$ cm.

TABLE II

DETECTOR SENSITIVITY (k) FOR DIFFERENT FLOW-RATES OF 0.1 M KNO_3 FOR 5-μl INJECTIONS OF VARYING CONCENTRATION OF $Cd(NO_3)_2$ SOLUTION

v^* (ml min^{-1})	$W_{1/2}$ (sec)	k	
		C l mol^{-1} × 10^3	A l mol^{-1} × 10^4
0.2	3.65	1.45	3.97
0.5	3.16	1.12	3.54
1.0	2.28	0.85	3.73
2.0	1.99	0.72	3.62
4.0	1.83	0.55	3.00

The mean sensitivity was $3.6 \cdot 10^{-4}$ A l mol^{-1} (10% relative standard deviation). In these measurements no damping was used in order to prevent additional peak broadening[5]. In Table II mean values of peak half-widths, $W_{1/2}$, are given for 5-μl injections of cadmium nitrate solution of varying concentration for different flow-rates of 0.1 M potassium nitrate solution. The mean standard deviation of the $W_{1/2}$ values is *ca.* 0.4 sec. As these peaks were recorded in the absence of a chromatographic column, they can also be assumed to be the measure of signal broadening.

After the mobile phase was stopped, residual current increased several-fold after a few minutes, presumbly owing to penetration of the oxygen-saturated solution of the reference electrode into the detection passage[10].

As the height of the chromatopolarographic signals recorded is dependent on the rate of mass transport, which in turn is dependent on flow-rate and drop time, we had to check how the peak area [h (μA) · $W_{1/2}$ (sec) = S (μC)] depends on flow-rate at different drop times. One would expect that for longer drop times, with an increase in electrolyte flow-rate, a convective transport component should manifest

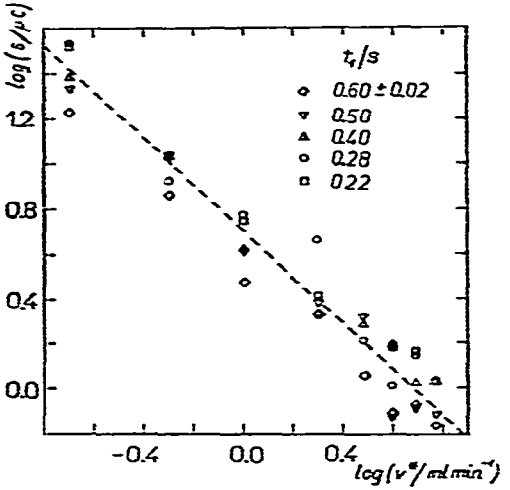

Fig. 9. Dependence of logarithm of peak surface area on flow-rate of 0.1 M KNO_3 solution for a 5-μl injected sample containing 10^{-3} M $Cd(NO_3)_2$ in 0.1 M KNO_3 solution without a chromatographic column for different mercury drop times: (●) 0.60; (×) 0.50; (△) 0.40; (○) 0.28; (□) 0.22 ± 0.02 sec.

itself to a greater extent on the recorded curves. This should lead to a relative increase in the peak currents at the same v^* in comparison with peak currents recorded for shorter drop times at which diffusion transport predominates. However, as can be seen in Fig. 9, the slope of the curves of logarithm of peak area versus logarithm of electrolyte flow-rate is almost independent on drop time in the range $0.22 \leqslant t_1 \leqslant 0.66$ sec and is equal to -1.02 with a relative standard deviation of 7% and a correlation coefficient of 0.98. This indicates a hyperbolic dependence of peak area on flow-rate and suggests that, independent of the drop time in the studied range, the peak area is reproducible only at a stable flow-rate.

Application

The detector was applied in the separation of a mixture of testosteroids to check its performance in the chromatographic system, and the results were compared with those obtained with the UV (254 nm) detector. Prior to this, polarograms of the reduction of testosterone and its homologues were taken with the use of both dropping (DME) and hanging mercury drop (HMDE) electrodes with a supporting electrolyte of the same composition as that of the electrolyte used in the chromatographic separation. All of the compounds studied showed the same polarographic behaviour and the polarogram and voltammogram of the reduction of 17α-methyltestosterone in 1/15 *M* phosphate buffer (pH 6)–acetonitrile (1:1) is presented in Fig. 10.

The polarograms revealed one broad hump, the height of which was directly proportional to the steroid concentration. Preliminary polarographic investigations indicated that the most suitable potential was -1.7 V *vs.* SCE. Such a negative

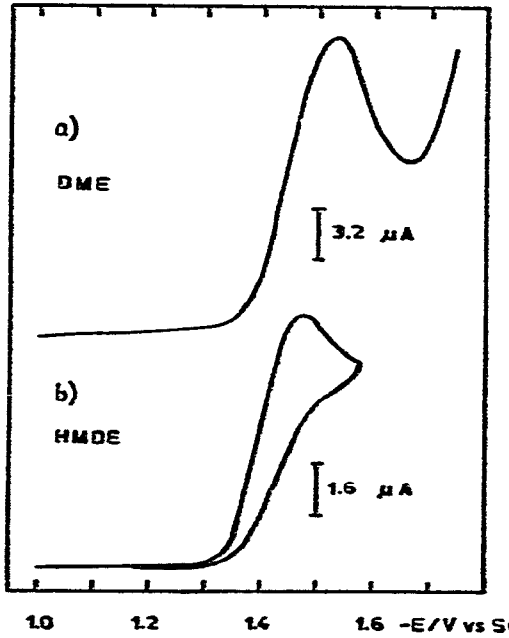

Fig. 10. Reduction curves for $5 \cdot 10^{-3}$ *M* 17α-methyltestosterone in solution containing 1/15 *M* phosphate buffer (pH 6)–acetonitrile (1:1) at (a) DME, $h_{Hg} = 110$ cm and (b) HMDE of surface area 1.78 mm², potential sweep rate 12.5 mV/sec.

potential is hardly available with a solid sensor electrode and in fact this excludes the possibility of using a voltametric detector.

Reversed-phase HPLC was used for the separation[38–42], and the results obtained with the two types of detector are shown in Figs. 11 and 12. LiChrosorb-RP 18 (10 μm) was used as the stationary phase, and the mobile phase was 1/15 *M* phosphate buffer (pH 6)–acetonitrile (1:1). Based on the analysis of the chromatograms obtained with the use of the UV (254 nm) detector, it was found that with an increase in flow-rate from 0.5 to 2.0 ml min^{-1} the partition function, R_s, and partition factor, α, of testosterone and 17α-methyltestosterone did not change significantly, *i.e.*, $R_s^{(0.5)} = 1.9$, $R_s^{(2.0)} = 1.5$; $\alpha^{(0.5)} = 1.36$, $\alpha^{(2.0)} = 1.34$. Therefore, studies with the use of the polarographic detector were carried out at a high flow-rate, 2 ml min^{-1}, in order to save time.

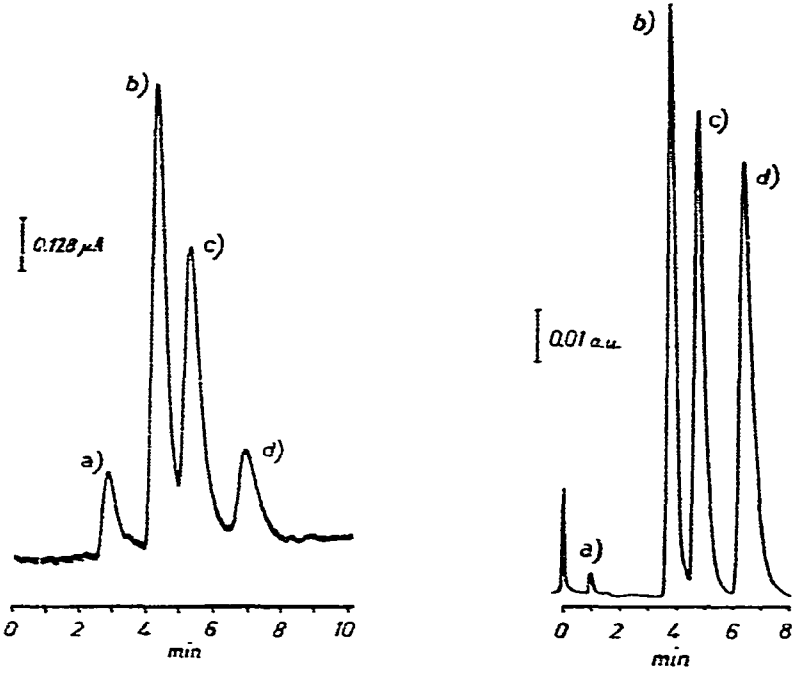

Fig. 11. HPLC of testosteroids mixture. Separation conditions: flow-rate, 2 ml/min; pressure, 75 kg cm^{-2}; stationary phase, LiChrosorb RP-18 (10 μm); column, stainless-steel, 250 × 4 mm I.D.; mobile phase, 1/15 *M* phosphate buffer (pH 6)–acetonitrile(1:1); drop time 0.3 sec; potentional, $E = -1.7$ V *vs.* SCE. (a) Oxygen; (b) 9.54 · 10^{-5} g of testosterone; (c) 9.96 · 10^{-5} g of 17α-methyltestosterone; (d) 10.43 · 10^{-5} g of 7β, 17α-dimethyltestosterone. The sample was partially deaerated with argon.

Fig. 12. HPLC of testosteroids mixture recorded with the use of the UV (254 nm) detector. Separation conditions as in Fig. 11. (a) Unknown; (b) 1.44 · 10^{-6} g of testosterone; (c) 1.51 · 10^{-6} g of 17α-methyltestosterone; (d) 1.58 · 10^{-6} g of 7β, 17α-dimethyltestosterone.

For the study of the reproducibility of the results obtained with both detectors, six consecutive injections were performed. The relative standard deviation of the peak height, h, was 7% and of the surface area, S ($S = W_{1/2}\,h$), 6% for both detectors.

A high value of the standard deviation for retention times resulted from the application of the stop-flow injection technique. The peak width at the foot recorded with the UV (254 nm) detector, $W \approx 2$ ml, was more than 20 times wider than its effective detection volume. This enables one to assume that the signal broadening is not caused by the detector. For the polarographic detector, W is on average 20% wider than that for the UV (254 nm) detector. However, as the effective detection volumes of the two detectors are comparable, this peak broadening does not result from greater sample diffusion in the polarographic detector. It may arise as a result of the high damping applied (setting damping No. 4 on the Radelkis OH-102 polarograph). This damping eliminated current oscillations due to the fall of the mercury drop. Therefore, one may suppose that better results would be obtained if tast-polarography with the application of electronic detection of the fall of the mercury drop was used.

The peak of oxygen dissolved in the injected sample was also recorded (Fig. 11). Its retention time is the shortest in this experiment. However, oxygen cannot be used as the marker of the column dead volume as it is retained on the bonded-phase column packing material, as demonstrated in Fig. 13. It can be seen that the sample of thallium nitrate solution injected into the same column under the same separation conditions before and after deaeration revealed a Tl^+ peak with shorter retention time than that of the oxygen peak.

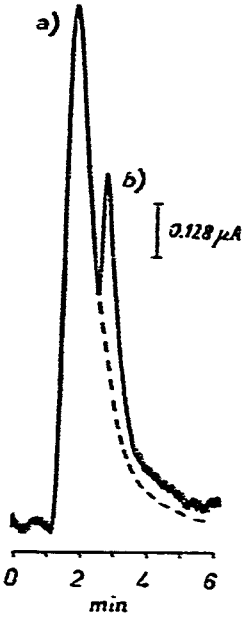

Fig. 13. HPLC of (a) $1.332 \cdot 10^{-5}$ g of $TlNO_3$ and (b) oxygen. Solid line, injected sample before deaeration with argon; broken line, after deaeration with argon. Separation conditions as in Fig. 11.

ACKNOWLEDGEMENTS

The authors thank Dr. A. Bylina for his assistance with the experiments and A. Kutner for help. This work was carried out within research project 03.10 of the Polish Academy of Sciences.

REFERENCES

1 W. Kemula, *Rocz. Chem.*, 26 (1952) 281.
2 C. D. Wilson and R. J. Smith, *Anal. Chem.*, 25 (1953) 218.
3 J. A. Lewis and K. C. Overton, *Analyst (London)*, 79 (1954) 293.
4 C. K. Mann, *Anal. Chem.*, 29 (1957) 1385.
5 G. J. Alkire, K. Koyama, K. J. Hahn and C. E. Michelson, *Anal. Chem.*, 30 (1958) 1912.
6 W. J. Blaedel and J. W. Todd, *Anal. Chem.*, 30 (1958) 1821.
7 R. L. Rebertus, R. J. Cappel and G. W. Bond, *Anal. Chem.*, 30 (1958) 1825.
8 C. P. Tyler and J. H. Karchmer, *Anal. Chem.*, 31 (1959) 499.
9 R. Tamamushi, S. Momiyama and N. Tanaka, *Anal. Chim. Acta*, 23 (1960) 585.
10 W. J.Blaedel and J. H. Strohl, *Anal. Chem.*, 33 (1961) 1631.
11 W. J. Blaedel and J. H. Strohl, *Anal. Chem.*, 36 (1964) 445.
12 E. B. Buchman and J. R. Bacon, *Anal. Chem.*, 39 (1967) 615.
13 R. P. Van Duyne and D. A. Aikens, *Anal. Chem.*, 40 (1968) 254.
14 M. Maruyama and M. Kakamoto, *Nippon Kagaku Kaishi*, (1976) 114.
15 J. G. Koen, J. F. K. Huber, H. Poppe and G. den Boef, *J. Chromatogr. Sci.*, 8 (1970) 192.
16 P. L. Joynes and R. J. Maggs, *J. Chromatogr. Sci.*, 8 (1970) 427.
17 Y. Takemori and M. Honda, *Rev. Polarogr.*, 16 (1970) 96.
18 E. Scarano, M. G. Bonicelli and M. Forina, *Anal. Chem.*, 42 (1970) 1470.
19 R. Stillman and T. S. Ma, *Microchim. Acta*, (1973) 491.
20 B. Fleet and C. J. Little, *J. Chromatogr. Sci.*, 12 (1974) 747.
21 T. Wasa and S. Musha, *Bull. Chem. Soc. Jap.*, 48 (1975) 2176.
22 W. Kemula, K. Butkiewicz and D. Sybilska, in T. Kambara (Editor), *Modern Aspects of Polarography*, Plenum Press, New York, 1966, p. 36.
23 W. Kemula, J. Stradiņš, I. Tutāne and D. Sybilska, in J. Stradiņš and S. Mairanovsky (Editors), *Polarographic Problems and Trends*, (in Russian), Zinātne, Riga, 1977; and references cited therein.
24 E. Pungor, K. Toth, Zs. Feher, C. Nagy and M. Varadi, *Anal. Lett.*, 8 (1975) ix.
25 P. T. Kissinger, *Anal. Chem.*, 49 (1977) 447A.
26 K. Brunt, *Pharm. Weekbl.*, 113 (1978) 689.
27 R. J. Davenport and D. C. Johnson, *Anal. Chem.*, 46 (1974) 1971.
28 W. Kemula, B. Behr, K. Chlebicka and D. Sybilska, *Rocz. Chem.*, 39 (1965) 1315.
29 Z. Borkowska, D. Sybilska and B. Behr, *Rocz. Chem.*, 45 (1971) 269.
30 W. Kemula, B. Behr, Z. Borkowska and J. Dojlido, *Collect. Czech. Chem. Commun.*, 30 (1965) 4050.
31 J. Lankelma and H. Poppe, *J. Chromatogr. Sci.*, 14 (1976) 310.
32 R. J. O'Halloran, J. C. Schaar and D. E. Smith, *Anal. Chem.*, 50 (1978) 1073, and references cited therein.
33 A. Bylina, K. Leśniak and S. Romanowski, *J. Chromatogr.*, 148 (1978) 69.
34 W. Kutner, J. Dębowski and W. Kemula, *Polish Pat.*, Appl. No. P 21062, 1978.
35 I. Smoler, *Chem. Zvesti*, 8 (1955) 867.
36 H. Svensson, *Anal. Chem.*, 25 (1953) 913.
37 Z. Galus, *Fundamentals of Electrochemical Analysis*, Wiley, New York, 1977.
38 F. Bailey, *J. Chromatogr.*, 122 (1976) 73.
39 M. J. O'Hare, E. C. Nice, R. Magee-Brown and H. Bullman, *J. Chromatogr.*, 125 (1976) 357.
40 B. B. Wheals and I. Jane, *Analyst (London)*, 102 (1977) 625.
41 Z. Deyel, K. Macek and J. Janak (Editors), *Liquid Column Chromatography, A Survey of Modern Techniques and Applications*, Elsevier, Amsterdam, Oxford, New York, 1975.
42 E. Heftman, *Chromatography of Steroids*, Elsevier, Amsterdam, Oxford, New York, 1976.